Hyperfine Interact (2016) 237: 122
DOI 10.1007/s10751-016-1337-y

Present status of the ^{129}Xe comagnetometer development for neutron EDM measurement

M. Mihara[1] · Y. Masuda[2] · K. Matsuta[1] · S. Kawasaki[2] · Y. Watanabe[2] · K. Hatanaka[3] · R. Matsumiya[3]

Published online: 10 August 2016

Abstract A ^{129}Xe comagnetometer designed for the measurement of neutron electric dipole moment (nEDM) as precisely as 1×10^{-27} e cm is presented. Highly nuclear spin polarized ^{129}Xe are introduced into an EDM cell where the ^{129}Xe spin precession is detected by means of the two-photon transition. The geometric phase effect (GPE) which generates the false nEDM was quantitatively discussed and the systematic error of nEDM from the GPE was estimated considering the buffer-gas suppression due to Xe atomic collisions. Research and development are in progress to construct the ^{129}Xe comagnetometer with a field sensitivity of 0.3 fT. At present, about 70 % nuclear spin polarized ^{129}Xe atoms have been obtained in a spin exchange opitial pumping cell, that are in the process of being transferred into the EDM cell via a cold trap.

Keywords Neutron electric dipole moment · ^{129}Xe comagnetometer · Geometric phase effect · Two-photon transition · Optical pumping

1 Introduction

The neutron electric dipole moment (nEDM) has been providing strict constraints on new physics underlying the CP violation that predict larger nEDM than the standard model. In

This article is part of the Topical Collection on *Proceedings of the International Conference on Hyperfine Interactions and their Applications (HYPERFINE 2016), Leuven, Belgium, 3-8 July 2016*

✉ M. Mihara
mihara@vg.phys.sci.osaka-u.ac.jp

[1] Department of Physics, Osaka University, 1-1, Machikaneyama, Toyonaka, Osaka 560-0043, Japan

[2] High Energy Accelerator Research Organization (KEK), Institute of Particle and Nuclear Studies (IPNS), 1-1, Oho, Tsukuba, Ibaraki 305-0801, Japan

[3] Research Center for Nuclear Physics (RCNP), Osaka University, 10-1, Mihogaoka, Ibaraki, Osaka 567-0047, Japan

order to exceed the present upper limit on the nEDM of 2.9×10^{-26} e cm (90 % C. L.) measured at the Institut Laue-Langevin (ILL) [1], many institutes are now developing new methods of nEDM measurements. For the nEDM measurement of 1×10^{-27} e cm, we have developed a new ultra cold neutron (UCN) source of superfluid helium (He-II) in a spallation neutron source [2, 3] to increase the UCN density in an EDM measurement cell, which leads to reduce the statistical error in the nEDM measurement. Another important issue is to reduce the systematic error, which was dominated by the geometric phase effect (GPE) for the ^{199}Hg comagnetomter at the ILL experiment. We have proposed a ^{129}Xe buffer-gas comagnetometer [4] which can reduce the systematic error from the GPE to 1×10^{-27} e cm. The basic design and the progress of our development for the ^{129}Xe comagnetometer are presented.

2 Outline of ^{129}Xe comagnetometer

The nEDM is measured by means of the Ramsey resonance in which the difference in the neutron Larmor frequency ω_n between a static electric field $\mathbf{E}$ parallel and anti-parallel to the static magnetic field $\mathbf{B}_0$ in the EDM cell. In order to compensate the drift and the changes of $\mathbf{B}_0$ during $\mathbf{E}$ reversals, spin polarized ^{129}Xe is introduced into the EDM cell and the Larmor frequency ω_{Xe} of the ^{129}Xe nuclear spin is precisely measured simultaneously with the neutron Ramsey resonance. Here, the nEDM d_n is represented using the Larmor frequency ratio $\omega_n/\omega_{\mathrm{Xe}}$ by

$$d_n \approx \frac{\hbar\omega_n}{4E}\left\{1 - \frac{(\omega_n/\omega_{\mathrm{Xe}})_{E_+}}{(\omega_n/\omega_{\mathrm{Xe}})_{E_-}}\right\} + \frac{\gamma_n}{\gamma_{\mathrm{Xe}}} d_{\mathrm{Xe}} - (d_{n\mathrm{f}} - d_{n\mathrm{Xef}}) \tag{1}$$

where, $(\omega_n/\omega_{\mathrm{Xe}})_{E_\pm}$ is the ratio when the electric field is parallel (E_+) or anti-parallel (E_-) to $\mathbf{B}_0$. d_n is determined by the correction for the ^{129}Xe EDM d_{Xe} multiplied by the ratio of gyromagnetic ratios $\gamma_n/\gamma_{\mathrm{Xe}}(= 2.459)$ for neutron and ^{129}Xe, and for the false nEDM $d_{n\mathrm{f}}$ and $d_{n\mathrm{Xef}}$ arising from the GPE for neutron and ^{129}Xe, respectively. For the d_n measurement of 1×10^{-27} e cm, required precision $\delta\omega_{\mathrm{Xe}}/2\pi$ is 4 nHz at $E = 10$ kV/cm, which corresponds to a magnetic field sensitivity δB of 0.3 fT. The most precise measurement of the ^{129}Xe EDM gives the upper limit of $(\gamma_n/\gamma_{\mathrm{Xe}})d_{\mathrm{Xe}} = 1 \times 10^{-26}$ e cm [5]. However, this value is expected to be the order of 10^{-29} e cm from the most strict experimental limit of an atomic EDM of 3.1×10^{-29} e cm for ^{199}Hg [6]. The GPE causes the systematic error as the false nEDM, which will be discussed in Section 3.

Schematic view of the ^{129}Xe comagnetometer which we are now developing is shown in Fig. 1. The ^{129}Xe nuclear spin is highly polarized far beyond the thermal equilibrium (hyperpolarized) by means of the spin exchange optical pumping (SEOP) applying to the Rb-^{129}Xe system, where nitrogen gas is included as a buffer gas for radiation quenching [7]. We are developing a freeze-pump-thaw method [8] to remove the nitrogen gas which induces UCN losses in the EDM cell due to the neutron absorption and up scattering by ^{14}N. The polarized ^{129}Xe gas is frozen in a cold trap, and then the nitrogen gas is pumped out from the trap. After removing the nitrogen gas, the trap is warmed up so that polarized ^{129}Xe atoms are transferred to the EDM cell. The ^{129}Xe polarization which is initially parallel to $\mathbf{B}_0$ is rotated by applying a $\pi/2$ RF pulse and start precession in the xy plane as in the case of the neutron Ramsey resonance. At present, we have achieved the ^{129}Xe polarization of about 70 % in the SEOP cell, which will be presented in Section 4.

Detection of the ^{129}Xe nuclear spin precession in the EDM cell using the two-photon transition of ^{129}Xe atom is being planned, which was first proposed by T.E. Chupp et al. [9].

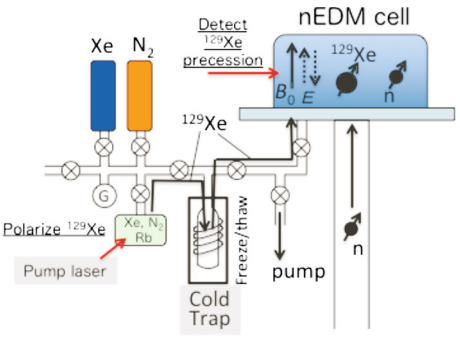

Fig. 1 Schematic design of the ^{129}Xe comagnetometer

The $5p^6(^1S_0)$ ground state of ^{129}Xe atom has a total angular momentum F of 1/2 due to the ^{129}Xe nuclear spin $I = 1/2$. The $5p^5 6p(^2[3/2]_2)$ state (9.821 eV) is excited from the ground state upon two photons absorption of a wavelength λ of 252.5 nm [10]. This excited level splits into two levels of $F = 3/2$ and 5/2 by the hyperfine interactions with a level spacing of 2 GHz [11]. If only a transition to the $F = 3/2$ level is induced with circularly polarized (σ_+) light, only $M_F = -1/2$ of the ground state is allowed to absorb two photons according to the selection rule of $\Delta M_F = +2$. Therefore, the σ_+ photons incident continuously on the EDM cell perpendicular to the z axis can selectively excite ^{129}Xe atoms with the nuclear spin direction of anti-parallel to the light axis. By detecting the succeeding fluorescence which is in infrared (IR) with $\lambda = 823$ or 895 nm [12], the ^{129}Xe nuclear spin precession can be observed as oscillating photon counts as a function of time.

In order to realize $\delta B \leq 0.3$ fT, ^{129}Xe polarization of higher than 50 % in the EDM cell and a continuous wave (CW) laser at $\lambda = 252.5$ nm with a power of higher than 0.5 mW are required. Details of the statistical estimation for the detection of ^{129}Xe precession in the EDM cell will be discussed in Section 5.

3 Geometric phase effect

Particles in the EDM cell see transverse magnetic fields $(\partial B_{0z}/\partial z)\mathbf{r}/2$ and $\mathbf{E}\times\mathbf{v}/c^2$ originating from the magnetic field gradient $\partial B_{0z}/\partial z$ and particle motion in $\mathbf{E}$, respectively, which rotate as the particle moves in the EDM cell. The effect of these rotations is represented in terms of time dependent perturbations, namely Dyson series [4]. While $\mathbf{E}$ dependence in the 1st order term is cancelled after integration with time, the 2nd order term remains and induces a false EDM effect, which is called the geometric phase effect.

Pendlebury et al. studied the GPE for UCN and comagnetometer spins in a cylindrical cell [13]. UCN spins are in the adiabatic regime ($\omega_r/\omega_n \ll 1$), at a typical magnetic field B_{0z} of 1 μT which gives $\omega_n/2\pi = 29$ Hz and a UCN rotation frequency $\omega_r/2\pi = \langle v_{xy}\rangle/(2\pi R) = 3.8$ Hz in the EDM cell, where $\langle v_{xy}\rangle$ is the root mean square velocity in xy plane, which is 2.4 m/s for UCN, and the EDM cell radius $R = 0.1$ m. The false nEDM d_{nf} arising from the GPE for neutrons is then represented by

$$d_{nf} = -(\hbar/4)(\partial B_{0z}/\partial z)(1/B_{0z}^2)(\langle v_{xy}\rangle^2/c^2). \tag{2}$$

If we achieve $\partial B_{0z}/\partial z = 0.1$ nT/m, $|d_{nf}| = 1 \times 10^{-28}$ e cm is obtained.

For the ^{129}Xe comagnetometer, the GPE is expressed in the non-adiabatic regime ($\omega_r/\omega_{Xe} \gg 1$), because $\omega_{Xe}/2\pi = 12$ Hz and $\omega_r/2\pi = 310$ Hz with $\langle v_{xy}\rangle = 196$ m/s. The

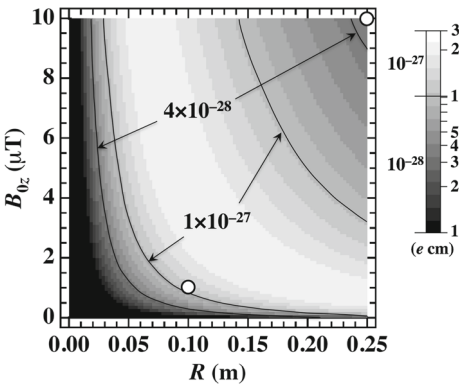

Fig. 2 False nEDM $d_{n\mathrm{Xef}\lambda}$ arising from GPE for ^{129}Xe nuclear spin as functions of B_0 and R. The ratio $(\partial B_{0z}/\partial z)/B_{0z}$ is kept at (0.1 nT/m)/μT. $\lambda_{\mathrm{Xe}} = 10$ mm and $\langle v_{xy}\rangle = 196$ m/s were used in the calculation. The *open circles* indicate conditions intended to achieve

false nEDM $d_{n\mathrm{Xef}}$ for the ^{129}Xe GPE is represented by

$$d_{n\mathrm{Xef}} = (\hbar/8)\,|\gamma_n\gamma_{\mathrm{Xe}}|\,(\partial B_{0z}/\partial z)(R^2/c^2). \tag{3}$$

Because of a small neutron cross section for ^{129}Xe, the ^{129}Xe atomic number density can be much increased compared with ^{199}Hg (http://www.nndc.bnl.gov/exfor/endf00.jsp). This allows that the position-velocity correlation in the **E** dependent term is suppressed during random walks of ^{129}Xe atoms due to collisions [4]. According to the studies of discharge, we assume a ^{129}Xe pressure of 3 mTorr, which gives a ^{129}Xe mean free path λ_{Xe} of 10 mm [14], where we can apply $E = 10$ kV/cm for a 10 cm gap of the EDM cell [3, 4]. Pendlebury et al. showed the suppression factor is expressed in terms of the ratio of the Larmor precession period $2\pi/\omega_{\mathrm{Xe}}$ to the diffusion period $(2R)^2/(\langle v_{xy}\rangle\lambda_{\mathrm{Xe}})$ [13], and then the false nEDM with a buffer gas effect $d_{n\mathrm{Xef}\lambda}$ is represented by

$$d_{n\mathrm{Xef}\lambda} = 1/\left[1 + [(2\pi/\omega_{\mathrm{Xe}})/\{(2R)^2/(\langle v_{xy}\rangle\lambda_{\mathrm{Xe}})\}]^{-2}\right] \times d_{n\mathrm{Xef}}. \tag{4}$$

To examine possible conditions of B_{0z}, R and $\partial B_{0z}/\partial z$, a coutour plot of $d_{n\mathrm{Xef}\lambda}$ was made as functions of B_{0z} and R which is shown in Fig. 2. Here, the ratio of the field gradient to the field strength $(\partial B_{0z}/\partial z)/B_{0z}$ is kept constant at (0.1 nT/m)/μT. Under the condition of $R =$ 0.1 m, $B_{0z} = 1$ μT, and $\partial B_{0z}/\partial z = 0.1$ nT/m, $d_{n\mathrm{Xef}\lambda}$ is estimated to be 1.2×10^{-27} e cm. If we increase R and B_{0z} to 0.25 m and 10 μT, respectively, the buffer-gas effect becomes remarkable and $d_{n\mathrm{Xef}\lambda}$ is suppressed to 0.3×10^{-27} e cm even at $\partial B_{0z}/\partial z = 1$ nT/m.

4 Production of hyperpolarized ^{129}Xe

We have constructed an apparatus shown in Fig. 3 for the SEOP to generate hyperpolarized ^{129}Xe and report on the measurements of ^{129}Xe polarization P_{Xe} in a SEOP cell. A 20-mmϕ spherical glass cell containing a small amount of Rb drop was connected to a gas handling system through a joint between glass and stainless steel tubing and a valve to make Xe and N_2 pressures variable. The inner surface of the cell was chemically cleaned in advance according to the procedure presented in ref. [15]. Circular polarized light of 795 nm provided by a laser diode array irradiated the cell to induce the D1 transition and polarize Rb atoms. The laser line width was narrowed to a few one-tenth nm using a grating with 2400 lines/mm to form an external cavity [16]. The laser power before the cell was about 8 W and the beam size was 25 × 25 mm. The cell was confined in an oven made of fluoroplastics to control the cell temperature that is the Rb vapor pressure by flowing hot nitrogen gas. An

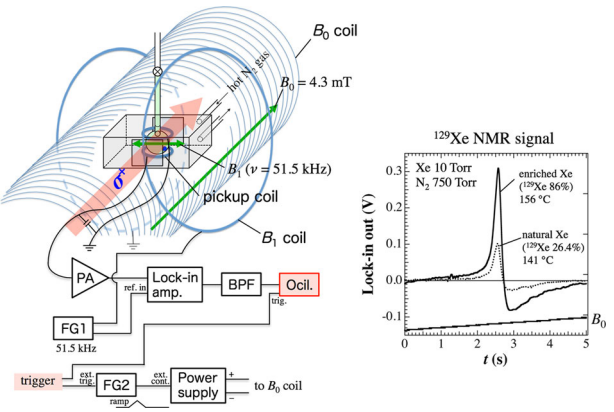

Fig. 3 Equipments of the Rb-Xe spin exchange optical pumping and AFP-NMR. A ^{129}Xe NMR signal is detected by a pickup coil that is processed via a lock-in amplifier. Typical NMR signals are also shown

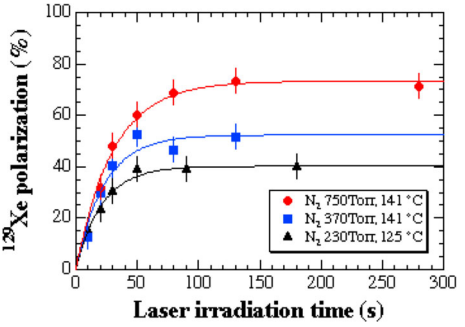

Fig. 4 Laser irradiation time dependence of ^{129}Xe spin polarization generated by means of the spin exchange optical pumping

external field B_0 of 4.3 mT was applied at the cell along the laser axis and P_{Xe} transferred from Rb polarization in the cell was measured by means of an adiabatic fast passage (AFP) NMR, which induce inversion of ^{129}Xe polarization under modulated B_0 and generates an NMR signal as shown in Fig. 3. The ^{129}Xe NMR signals were calibrated to deduce P_{Xe} by a proton NMR signal using a glass cell which contains distilled water and is the same size as the SEOP cell.

P_{Xe} exhibits buildup and saturation after continuous laser irradiation as typical $P_{Xe}(t)$ curves as a function of the laser irradiation time t are shown in Fig. 4, which is expressed by $P_{Xe}(t) = \gamma_{SE}/(\gamma_{SE} + \Gamma_w) P_{Rb}\{1 - e^{-(\gamma_{SE}+\Gamma_w)t}\}$ [15], where γ_{SE} is Rb-^{129}Xe spin exchange rate and Γ_w is the ^{129}Xe nuclear spin relaxation rate due to interaction at the wall. The Rb atomic polarization P_{Rb} is dominated by the optical pumping rate and the Rb atomic spin destruction rate that compete with each other. In order to search for a condition to maximize P_{Xe} in the SEOP cell, we have examined saturated polarization $P_{Xe}(\infty)$ as a function of nitrogen pressure p_{N_2} with the fixed natural Xe pressure at 10 Torr by measuring P_{Xe} at $t = 200 - 300$ s that can be assumed to be fully saturated since P_{Xe} mostly saturates within several tens seconds as shown in Fig. 4. The optimum cell temperature at each condition was determined in order that the maximum $P_{Xe}(\infty)$ value could be obtained. The result is summarized in Table 1, which shows that $P_{Xe}(\infty)$ becomes higher with increasing p_{N_2} and reached 70 % at $p_{N_2} = 750$ Torr. This means the ^{129}Xe collision rate at the wall becomes

Table 1 Summary of saturated ^{129}Xe polarization generated in the SEOP cell after laser irradiation for 200−300 s under some Xe and N_2 gas mixture conditions

Xe (Torr)	N_2 (Torr)	optimum temperature (°C)	P_{Xe} (%)
10	230	125	42
10	370	135	59
10	750	140	71
10[a]	750	155	68

[a]86 % enriched ^{129}Xe gas was used. For the others natural Xe was used

Table 2 Summary of conditions that we are planning for the fluorescence detection via the ^{129}Xe two-photon transition

Two-photon cross section $\sigma_{tot}(5p^6 \rightarrow 5p^5 6p)$	1.7×10^{-35} cm^4 [10]
Doppler broadening $\Delta\omega_D/2\pi$ (FWHM)	1.3 GHz
Laser power P	500 mW
Laser photon energy $\hbar\omega$	4.91 eV (252.5 nm)
Laser beam radius r_0	50 μm
^{129}Xe number density n_{Xe}	1.1×10^{14} cm^{-3} (3 mTorr)
Sensitive length to fluorescence detection L	10 cm
Fraction of photo ionization F_{pi}	∼0.001
Efficiency of fluorescence detection ε_f	1 %
Averaged fluorescence counting rate $\overline{n_f}$	1×10^8 s^{-1}

The averaged fluorescence counting rate is expressed by $\overline{n_f} = \sigma_{tot}(\sqrt{2ln2/\pi}/\Delta\omega_D)(P/\hbar\omega)^2(1/\pi r_0^2)n_{Xe}L(1-F_{pi})\varepsilon_f$ [10]

smaller with increasing p_{N_2}, which results in reducing Γ_w without changing γ_{SE}. Nearly the same P_{Xe} was obtained at $p_{N_2} = 750$ Torr even for 86 % enriched ^{129}Xe gas as that for natural Xe gas containing 26.4 % of ^{129}Xe. The present $P_{Xe}(\infty)$ value of about 70 % is comparable to the previous works by similar methods to ours [8, 17], and should be enough to maintain P_{Xe} higher than 50 % during transfer to the EDM cell.

Further studies are in progress for increasing the number of polarized ^{129}Xe atoms using a larger SEOP cell and constructing the ^{129}Xe transfer system via a cold trap.

5 Statistical estimation

The ^{129}Xe nuclear spin precession is observed using the detection of fluorescence accompanied by the two-photon transition of ^{129}Xe atoms during the free precession period T in the neutron Ramsey resonance measurement. The ^{129}Xe Larmor frequency ω_{Xe} is determined from the the fluorescence counting rate n_f as a function of time t after the end of $\pi/2$ pulse, which is described as $n_f(t) = \overline{n_f} P_{Xe} \cos(\omega_{Xe} t + \phi) e^{-t/T_2}$, where $\overline{n_f}$ is the averaged fluorescence counting rate, P_{Xe} is the initial ^{129}Xe polarization in the EDM cell, and T_2 is the transverse relaxation time for ^{129}Xe nuclear spin. Required statistics of the fluorescence counts n_f to achieve $\delta\omega_{Xe}/2\pi = 4$ nHz, i.e. $\delta B = 0.3$ fT, were estimated to be 1×10^{13} in total, assuming $T = 130$ s [1], $T_2 = 300$ s, and $P_{Xe} = 0.5$. The fluorescence yield was

estimated based on the study on the two-photon absorption cross section of Xe atoms to the $5p^5 6p(^2[3/2]_2)$ state [10], which is summarized in Table 2. To induce the two-photon transition, we are considering an ultra violet (UV) continuous wave (CW) 252.5-nm laser using $CsLiB_6O_{16}$ (CLBO) or β-BaB_2O_4 (BBO) as a nonlinear optical crystal for the second harmonics generation. As the result, $\overline{n_f}$ of 1×10^8 s^{-1} is expected if we use a CW 252.5-nm laser with a power of 500 mW. This indicates that the fluorescence counts obtained during the duration of a Ramsey cycle ($T = 130$ s) becomes about 10^{10} that gives the sensitivity $\delta B \sim 10$ fT. Thus we can achieve $\delta B = 0.3$ fT by averaging over $\sim 10^3$ Ramsey cycles.

6 Summary

A plan of the ^{129}Xe comagnetometer being developed for applying to the precise nEDM measurement was presented. Highly spin polarized ^{129}Xe generated by means of the optical pumping are introduced into the EDM cell through a cold trap. The ^{129}Xe spin precession in the EDM cell is detected using the two-photon transition during the neutron Ramsey resonance measurement. The quantitative discussion of the GPE for ^{129}Xe showed that a false nEDM of 1×10^{-27} e cm is achievable under an nEDM measurement condition with $R = 0.1$ m, $B_{0z} = 1$ μT, and $\partial B_{0z}/\partial z = 0.1$ nT/m at a Xe pressure of 3 mTorr and it can be reduced to 0.3×10^{-27} e cm with increasing R, B_{0z}, and $\partial B_{0z}/\partial z$ to 0.25 m, 10 μT, and 1 nT/m, respectively, where the buffer gas suppression is more remarkable. A field sensitivity of $\delta B = 0.3$ fT is expected by accumulating the fluorescence counting statistics with about 10^3 Ramsey cycles when we obtain 50 % polarized ^{129}Xe and a CW 252.5-nm laser with a power of $\sim$500 mW. About 70 % of ^{129}Xe polarization has been achieved in the SEOP cell and further research and development are in progress to construct the ^{129}Xe comagnetometer we presented in this paper.

Acknowledgments This work was supported by JSPS KAKENHI Grant Number JP 21224007.

References

1. Baker, C., Doyle, D., Geltenbort, P., Green, K., van der Grinten, M., Harris, P., Iaydjiev, P., Ivanov, S.N., May, D.J.R., Pendlebury, J.M., Richardson, J., Shiers, D., Smith, K.: Phys. Rev. Lett. **97**, 131801 (2006)
2. Masuda, Y., Hatanaka, K., Jeong, S.C., Kawasaki, S., Matsumiya, R., Matsuta, K., Mihara, M., Watanabe, Y.: Phys. Rev. Lett. **108**, 134801 (2012)
3. Masuda, Y., Hatanaka, K., Jeong, S.C., Kawasaki, S., Matsumiya, R., Matsuta, K., Mihara, M., Watanabe, Y.: Phys. Procedia **51**, 89 (2014)
4. Masuda, Y., Asahi, K., Hatanaka, K., Jeong, S.C., Kawasaki, S., Matsumiya, R., Matsuta, K., Mihara, M., Watanabe, Y.: Phys. Lett. A **376**, 1347 (2012)
5. Rosenberry, M.A., Chupp, T.E.: Phys. Rev. Lett. **86**, 22 (2001)
6. Griffith, W.C., Swallows, M.D., Loftus, T.H., Romalis, M.V., Heckel, B.R., Fortsonx, E.N.: Phys. Rev. Lett. **102**, 101601 (2009)
7. Rosenberry, M.A., Reyes, J.P., Tupa, D., Gay, T.J.: Phys. Rev. A **75**, 023401 (2007)
8. Ruth, U., Hof, T., Schmidt, J., Fick, D., Jänsch, H.J.: Appl. Phys. B **68**, 93 (1999)
9. Alden, E.A., Degenkolb, S.M., Chupp, T.E., Leanhardt, A.E.: Bulletin of the American Phys. Soc., 42nd Ann. Meeting of the APS DAMOP, 56, K2.00010 (2011)
10. Kröll, S., Bischel, W.K. Phys. Rev. A **41**, 1340 (1990)
11. D'Amico, G., Pesce, G., Sasso, A.: Hyperfine Interact. **127**, 121 (2000)
12. Horiguchi, H., Chang, R.S.F., Setser, D.W.: J. Chem. Phys. **75**, 1207 (1981)

13. Pendlebury, J.M., Heil, W., Sobolev, Y., Harris, P.G., Richardson, J.D., Baskin, R.J., Doyle, D.D., Geltenbort, P., Green, K., van der Grinten, M.G.D., Iaydjiev, P.S., Ivanov, S.N., May, D.J.R., Smith, K.F.: Phys. Rev. A **70**, 0.2102 (2004)
14. Haynes, W.M.: CRC Handbook of Chemistry and Physics, 91st edn, pp. 6–56. CRC Press/Taylor and Francis, Boca Raton (2010)
15. Rosen, M.S., Chupp, T.E., Coulter, K.P., Welsh, R.C.: Rev. Sci. Instr. **70**, 1546 (1999)
16. Masuda, Y., Ino, T., Stoy, V.R., Jones, G.L.: Appl. Phys. Lett. **87**, 053506 (2005)
17. Nikolaou, P., Coffy, A.M., Ranta, K., Walkup, L.L., Gust, B.M., Barlow, M.J., Rosen, M.S., Goodson, B.M., Chekmenev, E.Y.: J. Phys. Chem. B **118**, 4809 (2014)